View metadata, citation and similar papers at core.ac.uk

brought to you by CORE

provided by Elsevier - Publisher Connector

Physics Letters B 755 (2016) 58–63

Contents lists available at ScienceDirect

Physics Letters B

www.elsevier.com/locate/physletb

Lineshape of the Higgs boson in future lepton colliders ☆

S. Jadach [a], R.A. Kycia [b]

[a] The Henryk Niewodniczański Institute of Nuclear Physics, Polish Academy of Sciences, ul. Radzikowskiego 152, 31-342 Kraków, Poland
[b] T. Kościuszko Cracow University of Technology, Faculty of Physics, Mathematics and Computer Science, ul. Warszawska 24, 31-155 Kraków, Poland

ARTICLE INFO

Article history:
Received 13 November 2015
Received in revised form 30 January 2016
Accepted 30 January 2016
Available online 3 February 2016
Editor: L. Rolandi

Keywords:
QCD
The Higgs boson cross section
Energy scan
Centre-of-mass energy spread
Initial radiation state

ABSTRACT

The effect of the photon emission (initial-state radiation) in the cross section of the process of direct production of the Higgs boson in future high luminosity electron and muon colliders is calculated. It was found that the cross section at the top of the Higgs boson resonance peak is reduced by a factor 0.348 for the electron collider and 0.548 for the muon collider. A centre-of-mass energy spread of the centre-of-mass energy of 4.2 MeV (equal to the Higgs width) would reduce peak cross section further, by a factor 0.170 and 0.256 (QED and energy spread) for electron and muon beams respectively. Possible uncertainties in the resummed QED calculations are discussed. Numerical results for the lineshape cross section including QED and many values of the centre-of-mass energy spread are provided.

© 2016 The Authors. Published by Elsevier B.V. This is an open access article under the CC BY license (http://creativecommons.org/licenses/by/4.0/). Funded by SCOAP[3].

1. Introduction

The recent Higgs boson discovery at the CERN LHC [1–3] has initiated a new era of precision measurements of its properties. The measured Higgs boson mass, allows the observation and perhaps the study of its resonant production to be seriously considered at future electron or a dedicated muon colliders, via the processes $e^-e^+ \to H$ and $\mu^-\mu^+ \to H$. Due to the extremely small coupling of the Higgs boson to the electron, it seems at first sight that its direct production in the electron collider is just hopeless. However, in the Future Circular Collider with $e^\pm$ beams (FCCee) considered at CERN featuring very high luminosity, this process would in principle be observable, provided one could eliminate copious background processes. On the other hand, the stronger coupling of the Higgs to muons gives a dedicated muon collider a definite advantage, provided a decent luminosity and small centre-of-mass energy spread are achieved. In either case, centre-of-mass energy spread and an additional smearing of the beam energy due to QED initial-state radiation (ISR) are major points in the feasibility studies of these projects. This is why the present study was undertaken. The influence of the centre-of-mass energy spread on direct Higgs observation in a FCCee collider was already discussed at the 8th FCC-ee Physics Workshop [4]. In this work we shall concentrate mainly on calculating effects due to ISR of multiple photons. It is done using past experience in calculating very precisely the similar QED effect for Z boson production at LEP experiments, for instance in Ref. [5]. Similar analysis of the initial state QED corrections, taking into account the centre-of-mass energy spread, for $\mu^-\mu^+ \to H$ process can be also found[1] in Refs. [6] and [7].

The paper is organized as follows: After defining the Born cross section for Higgs production in lepton annihilation, we will discuss the effect of ISR corrections. We shall discuss theoretical uncertainties in the evaluation of this QED effect, presenting numerical results for three different QED ISR formulas, of varying sophistication level. The effect of the centre-of-mass energy spread in the cross section will be included in the discussion, presenting numerical results for several values of such a spread. Finally, analogous effects in planned muon colliders will be discussed and numerical results will be presented.

2. QED initial state radiation formulas

The Born cross section for the Higgs particle production in $e^\pm$ collider is given by the (relativistic [8]) Breit–Wigner (B-W) formula [5]

$$\sigma_B(s) = \frac{4\pi B_{ee}\Gamma_H^2}{(s-M_H^2)^2+\Gamma_H^2 M_H^2}, \tag{2.1}$$

☆ This work is partly supported by the Polish National Science Centre grant UMO-2012/04/M/ST2/00240.

E-mail address: rkycia@pk.edu.pl (R.A. Kycia).

[1] We thank M. Greco and S. Dittmaier for bringing these works to our attention.

http://dx.doi.org/10.1016/j.physletb.2016.01.065
0370-2693/© 2016 The Authors. Published by Elsevier B.V. This is an open access article under the CC BY license (http://creativecommons.org/licenses/by/4.0/). Funded by SCOAP[3].

where $M_H = 125.09$ GeV and $\Gamma_H = 4.2$ MeV according to Refs. [9–11]. The branching ratio of $e^+e^- \to H$ is $B_{ee} = 5.3 \cdot 10^{-9}$. The electron and muon branching ratios are related by the factor m_μ^2/m_e^2, thus the above result can be obtained from $B_{\mu\mu} = 2.19 \cdot 10^{-4}$; see also Refs. [10,11]. There are variants of the B-W formulas with an s-dependent width, but for a narrow resonance like the Higgs they differ negligibly from the above; see more discussion in the Appendix A.

The initial state radiation correction to this process was calculated using formulas of Ref. [5] for Z boson production.[2] The entire initial-state $\mathcal{O}(\alpha^2)_{prag}$ formula of the Ref. [5] integrated cross section reads:

$$\sigma_I(s) = \int_0^1 dv\ \rho_I(v)\sigma_B(s(1-v)),$$
$$\rho_I(v) = e^{\delta_{YFS}}\ F(\gamma)\ \gamma\, v^{\gamma-1}\ \{d_s + \Delta_H(v)\}, \tag{2.2}$$

where

I	d_s	$\Delta_H(v)$
(a)	1	0
(b)	$1+\frac{\gamma}{2}+A\frac{\alpha}{\pi}$	$v\left(-1+\frac{1}{2}\right)$
(c)	$1+\frac{\gamma}{2}+\frac{\gamma^2}{8}+A\frac{\alpha}{\pi}$	$v\left(-1+\frac{1}{2}\right)+\gamma\left[-\frac{v}{2}-\frac{1+3(1-v)^2}{8}\ln(1-v)\right]$

(2.3)

and

$$\delta_{YFS} = \frac{\gamma}{4} + \frac{\alpha}{\pi}\left(-\frac{1}{2}+\frac{\pi^3}{3}\right),$$
$$\gamma = 2\frac{\alpha}{\pi}\left(\ln\frac{s}{m_e^2}-1\right), \quad F(\gamma) = \frac{\exp(-C\gamma)}{\Gamma(1+\gamma)}. \tag{2.4}$$

Here, α is the QED coupling constant, m_e the electron mass and C is the Euler–Mascheroni constant. In the case of muon beams m_e in γ is replaced by m_μ and B_{ee} by $B_{\mu\mu}$.

The zero spin nature of the Higgs boson instead of spin one of the Z counts negligibly in the QED ISR effects, simply because the deformation of the resonance curve is mainly due to soft photons. The constant A which is responsible for the above spin difference is of order $\frac{\alpha}{\pi} \simeq 1/400$ without any logarithmic enhancement. It influences mainly an overall normalization – hence at the precision level we are aiming at, it can be safely set to zero.[3]

On the other hand, soft photon exponentiation/resummation in eq. (2.2) is critical and mandatory. The formula of eq. (2.2) comes from standard diagrammatic perturbative QED calculations including Yennie–Frautschi–Suura (YFS) exponentiation, see Ref. [5] and was originally introduced for the purpose of the algebraic validation of the Monte Carlo program YFS2 of Ref. [12]. Later on it was discussed and used in many papers; see for instance Refs. [5, 13–16] and the references therein.

The three variants (for $I = (a), (b)$ or (c)) of the ISR formula in eq. (2.2) correspond to the increasing sophistication (perturbative order) of the non-soft collinear radiative corrections. Changing the type of ISR formula will be used to estimate uncertainty due to unknown/neglected QED higher orders.

3. Centre-of-mass energy spread

In real accelerator experiments, the beam is not monoenergetic, i.e., centre-of-mass energy $E = \sqrt{s}$ has a spread δ around the centre value $E_0 = \sqrt{s_0}$ of the beam energy. The distribution of E is usually well approximated by the following Gaussian distribution:

$$G(E-E_0;\delta) = \frac{1}{\delta\sqrt{2\pi}} e^{-\frac{(E-E_0)^2}{2\delta^2}}. \tag{3.1}$$

Without QED effects, the Born cross section (2.1) gets simply convoluted with the energy spectrum of eq. (3.1):

$$\sigma_B^{conv}(E;\delta) = \int dE'\ \sigma_B(E')\ G(E'-E;\delta). \tag{3.2}$$

Once QED ISR is switched on, the following double convolution provides realistic experimental cross section:

$$\sigma_I^{conv}(E;\delta) = \int dE'\ \sigma_I(E') G(E'-E;\delta)$$
$$= \int dE' \int_0^1 dv \frac{1}{\delta\sqrt{2\pi}} e^{-\frac{(E'-E)^2}{2\delta^2}} \rho_I(v)\sigma_B(E'^2(1-v)), \tag{3.3}$$

for three variants, $I = (a), (b), (c)$ of the radiative function (2.2).

Because of the rapid decrease of the Gaussian distribution for large arguments, the energy integration range will be restricted to $E - 10\delta \le E' \le E + 10\delta$ without any loss of the calculation reliability. The numerical integrations in one and two dimensions require a little bit of care, because of strongly singular integrands. The adaptive integration library functions of ROOT library [17] were used. All results were also cross-checked using the FOAM adaptive Monte-Carlo simulator/integrator of [18–20].[4]

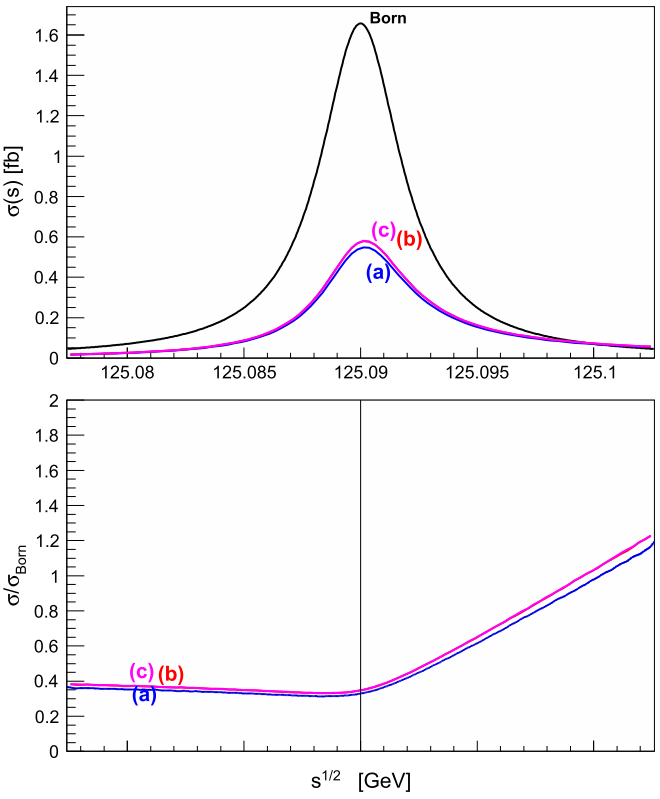

Fig. 1. Study of the pure QED effect in the Higgs line-shape for an electron collider. The plots show the Born cross section of eq. (2.1) and cross section affected by QED ISR, following eq. (2.2) for three types $I = a, b, c$ of the QED radiator functions defined in eq. (2.3). The ratios with respect to the Born cross section are also shown.

[2] See eq. (202) therein.

[3] Constant A is also set to zero in Ref. [7], while in Ref. [6] vertex and real-soft contributions are provided, but non-logarithmic constant A is explicitly obtained.

[4] Integration errors were also taken from FOAM, as they are more reliable.

Table 1
Born cross sections (in fb) of eq. (2.1) and three variants of the ISR-corrected cross sections of eq. (2.2) for three values of $\sqrt{s} = E = M_H = 125.09$ GeV and $E = M_H \pm \Gamma_H$ in the electron–positron collider. The integration error is below 0.0005 fb.

E	σ_B	$\sigma_{(a)}$	$\sigma_{(b)}$	$\sigma_{(c)}$	$\frac{\sigma_{(a)}}{\sigma_B}$	$\frac{\sigma_{(b)}}{\sigma_B}$	$\frac{\sigma_{(c)}}{\sigma_B}$
M_H	1.6573	0.5447	0.5748	0.5762	0.329	0.347	0.348
$M_H + \Gamma$	0.3315	0.1865	0.1971	0.1974	0.563	0.595	0.596
$M_H - \Gamma$	0.3315	0.1087	0.1147	0.1145	0.328	0.346	0.346

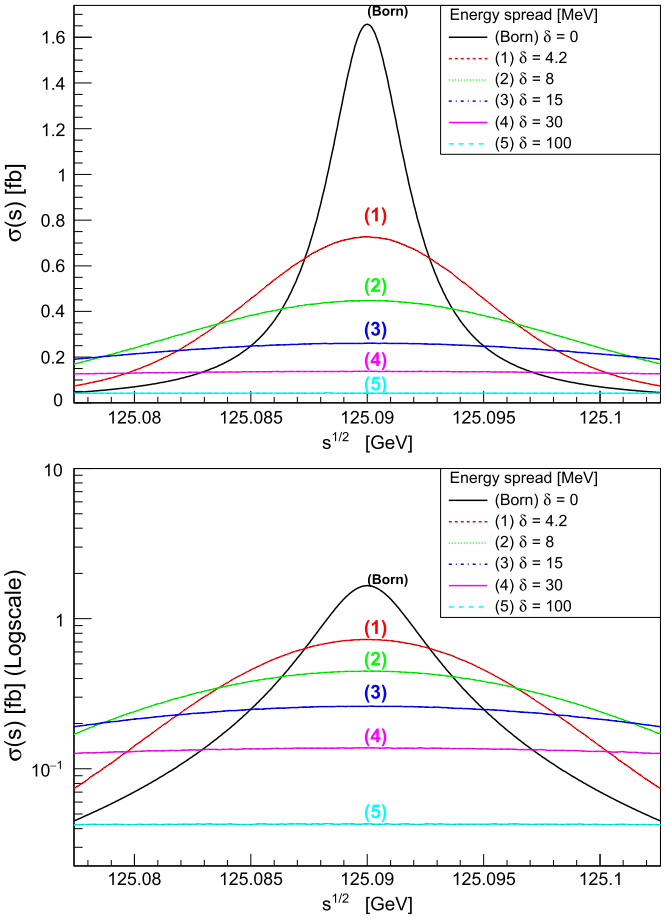

Fig. 2. Higgs production cross section in an electron–positron collider for several values of the centre-of-mass energy spread $\delta = 0, 4.2, 8, 15, 30, 100$ MeV. The QED ISR effect is not included. The second figure has logscale for better visibility.

4. Numerical results for electron–positron colliders

The Born cross sections and results from three variants of the ISR formula of eq. (2.2) are presented in Fig. 1. The cases $\sigma_{(b)}$ and $\sigma_{(c)}$ are almost indistinguishable. In addition, Table 1 presents the same results for the energy at the peak $E = M_H$ and near the peak $E = M_H \pm \Gamma_H$ with 4-digit precision. The QED uncertainty from unaccounted QED higher orders can be estimated from Table 1 looking into differences between ISR type $I = (c)$ and $I = (b)$. It is below 0.3% and is compatible with the estimate of neglected A in eq. (2.2) (it is also comparable to the numerical integration error). From now on we shall use the ISR formula for $I = (c)$ only.

The introductory exercise on the centre-of-mass energy spread is shown in Fig. 2 where the Higgs production cross section in the electron–positron collider is plotted without energy spread (Born) and for several values of the centre-of-mass energy spread $\delta = 4.2, 8, 15, 30, 100$ MeV. The QED ISR effect is not yet included.

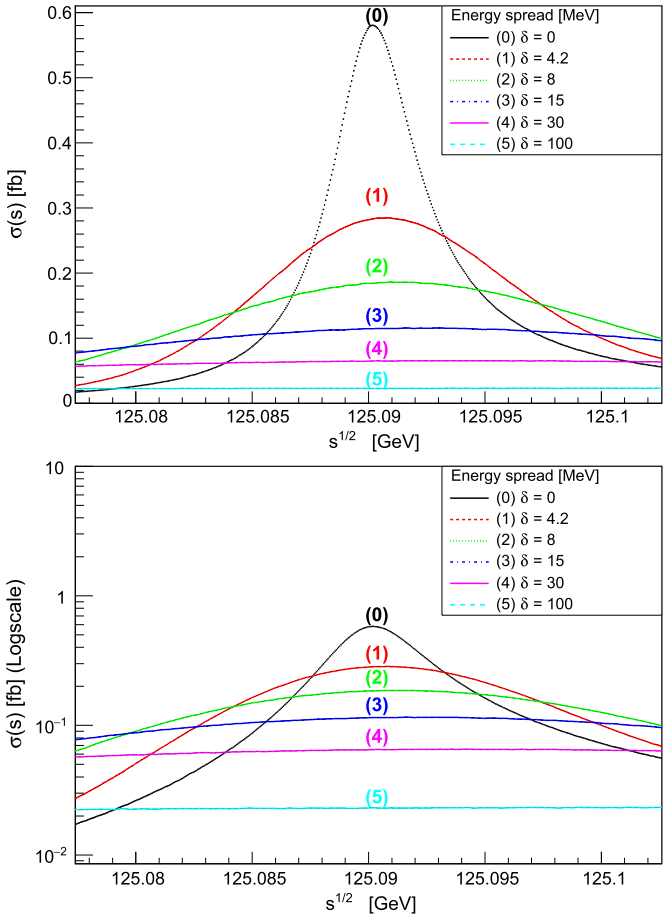

Fig. 3. Higgs production cross section in an electron–positron collider for several values of the centre-of-mass energy spread $\delta = 0, 4.2, 8, 15, 30, 100$ MeV. The QED ISR effect is included according to eq. (3.3), for ISR type (c). The second figure has logscale for better visibility.

On the other hand, Fig. 3 shows our most interesting result, the Higgs production cross section in an electron–positron collider including both the QED ISR effect according to eq. (3.3) for ISR type (c) and several examples of the centre-of-mass energy spread parameter $\delta = 4.2, 8, 15, 30, 100$ MeV.

In Fig. 4 we plot again the same Higgs production cross section in the electron–positron collider including both the QED ISR effect and centre-of-mass energy spread in the narrower energy range and for the energy spread parameter $\delta = 4.2$ MeV which is ambitiously aimed at the FCCee collider, and also for more realistic $\delta = 8.0$ MeV. The ratio of the cross section with respect to Born is also shown in the lower plot there.

The same results as in Fig. 4 are also shown in Table 2 for three values of the energy, at the resonance peak $E = M_H$ and near the peak $E = M_H \pm \Gamma_H$, with the 4-digit precision. As we see there, the combined reduction of the Higgs production process at the resonance peak due to QED effect is 0.348 and goes down to 0.170 for the centre-of-mass energy spread equal to the Higgs width ~ 4.2 MeV.

The suppression factor of the peak cross section due to QED ISR can be also quite well reproduced, and in this way cross checked, with a very simple approximate calculation presented in Appendix B. This approximation works even better in the case of the weaker ISR effect for muon beams.

The above results can be used as input for further studies of the practical observability of the Higgs resonant cross section in future electron–positron colliders.

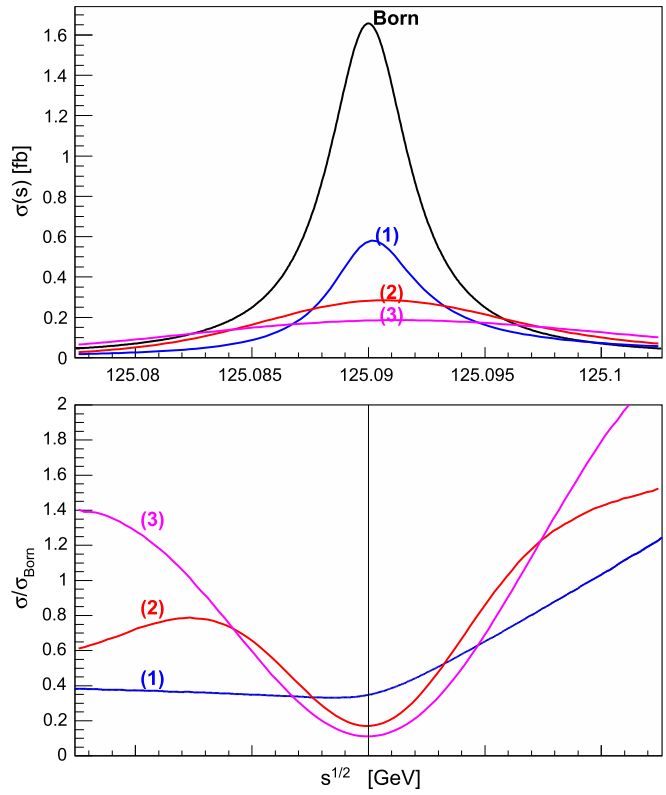

Fig. 4. Line-shape of the direct Higgs production process in an electro-positron collider including effect of ISR type (c) and the centre-of-mass energy spread. No energy spread is included (only ISR is on) in the line marked with (1), while the lines marked with (2) and (3) include ISR and energy spread $\delta = 4.2$ MeV and $\delta = 8.0$ MeV according to eq. (3.3). The reference Born cross section is also shown and the ratios with respect to Born are also plotted.

Table 2
Cross section of the direct Higgs production process in an electron–positron collider including the effect of ISR type (c) and the centre-of-mass energy spread. No energy spread is in $\sigma_{(1)}$, while $\sigma_{(2)}$ and $\sigma_{(3)}$ include ISR and energy spread $\delta = 4.2$ MeV and $\delta = 8.0$ MeV according to eq. (3.3). The reference Born cross section σ_B is also included and the ratios with respect to Born are also provided. The integration error is below 0.0005 fb.

E	σ_B	(1)	(2)	(3)	$\frac{(1)}{\sigma_B}$	$\frac{(2)}{\sigma_B}$	$\frac{(3)}{\sigma_B}$
M_H	1.6574	0.5762	0.2820	0.1841	0.348	0.170	0.111
$M_H + \Gamma$	0.3315	0.1974	0.2346	0.1774	0.596	0.708	0.535
$M_H + \Gamma$	0.3315	0.1145	0.1885	0.1559	0.346	0.569	0.470

In the above numerical exercises, we have used discrete values of the machine energy spread δ. In Fig. 5, we also show the continuous dependence on δ of the Higgs production process at the resonance peak, $E = M_H$, divided by the Born cross section, both for QED ISR switched on and off. More precisely, we are plotting there the following two ratios

$$\frac{\sigma_B^{conv}(M_H,\delta)}{\sigma_B(M_H)} \quad \text{and} \quad \frac{\sigma_{(c)}^{conv}(M_H,\delta)}{\sigma_B(M_H)}, \tag{4.1}$$

for ISR off and on respectively. ISR switched off case is obviously unphysical, however, it was placed in the plot as it can be helpful for those who want to recover the results as a cross-check.

One could easily expand the above numerical exercises to more values in the 2-dimensional space of the energy E and the centre-of-mass energy spread δ, but we think that the numerical results collected above are complete enough and can serve as a reliable starting point for all studies of the Higgs resonance observability in future electron–positron colliders.

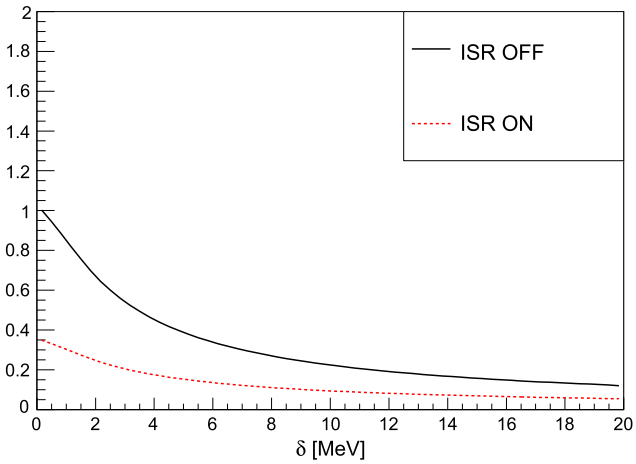

Fig. 5. The dependence of the Higgs production process at the resonance peak, $E = M_H$ in an electron–positron collider on the energy spread δ, divided by the Born cross section, for QED ISR switched on and off.

It is worth pointing out that because of the normalization of the convolution as a function of δ at $E = M_H$ to unity we can construct the following quantity that is close unity when δ/Γ_H is not too big. In Fig. 7, the following quantity

$$R_V(E,\delta) = \frac{\sigma_B^{conv}(E,\delta)}{\sigma_B(E)} \left(\frac{\sigma_{(c)}^{conv}(E,\delta)}{\sigma_{(c)}^{conv}(E,0)} \right)^{-1} \tag{4.2}$$

is plotted. If $R_V(E,\delta) \simeq 1$, then the double convolution can be replaced by the following handy approximation:

$$\sigma_{(c)}^{conv}(E,\delta) \simeq \sigma_{(c)}^{conv}(E,0)\, \frac{\sigma_B^{conv}(E,\delta)}{\sigma_B(E)}.$$

As seen in Fig. 7 the above approximation for $E = M_H$ works reasonably, within 10% for $\delta \le \Gamma_H$, but its validity deteriorates significantly for $\delta > \Gamma_H$ and in such a case numerical double convolution is unavoidable.

5. Numerical results for muon colliders

The calculations of the previous section can be easily extended to the case of a muon collider, in the so-called Higgs factories (for overview see, e.g., [21]), by means of replacing m_e with m_μ and B_{ee} with $B_{\mu\mu}$ in the equations of section 2 (see also [6] or [7]). This kind of collider will produce a clean sample of Higgs boson without much background and therefore would allow the Higgs mass and its properties to be measured very precisely. Our analysis is vital in view of MAP (Muon Accelerator Program) [21] at Fermilab and the new ideas of producing muon monochromatic beams, that would limit the major obstacle, the centre-of-mass energy spread.

Thanks to the much higher branching ratio for the Higgs to a muon pair, the production cross section for $\mu^+\mu^- \to H$ is much higher. Also, QED effects for muon collider are roughly a factor 2 weaker, simply because for the muon beams at the Higgs peek, $\gamma = 0.0611$, as compared to $\gamma = 0.1106$ for electron beams.

Numerical results for a muon collider are presented in Fig. 6 and Table 3, and correspond to Higgs production cross section dependence on energy E and machine energy spread δ shown in Fig. 4 and in Table 2. As seen in this table, the reduction factor of the cross section at the resonance peak due to QED ISR is now only 0.548. For the centre-of-mass energy spread $\delta = 8$ MeV, it deteriorates down to 0.163 (which is accidentally comparable to

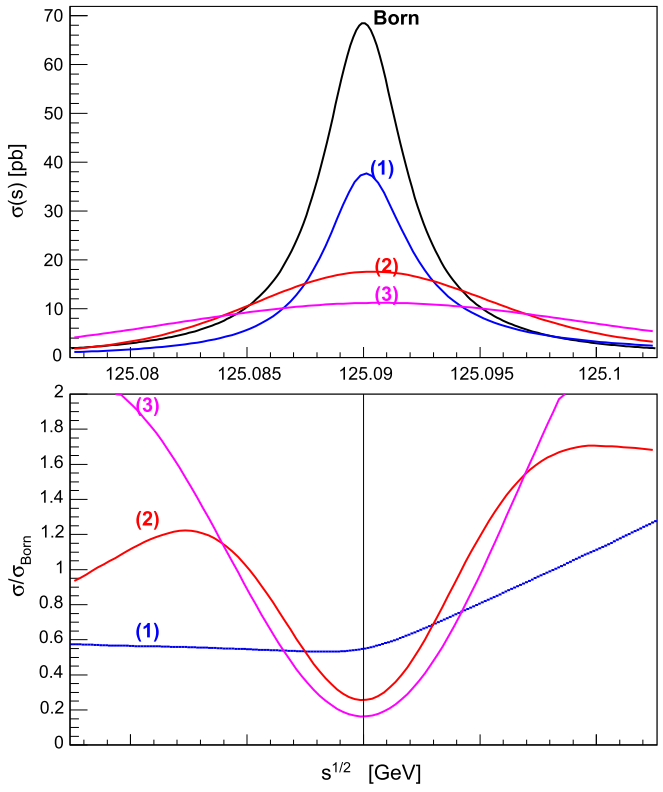

Fig. 6. Line-shape of the direct Higgs production process in an $\mu^+\mu^-$ collider including the ISR effect and the centre-of-mass energy spread. The input and notation are as in Fig. 4.

Table 3
Cross section of the direct Higgs production process in the $\mu^+\mu^-$ collider including effect of ISR type (c) and the centre-of-mass energy spread. The same values of the energy spread δ an energy E are used as in Table 2. The Monte Carlo integration error is below 0.03 pb.

E	σ_B	(1)	(2)	(3)	$\frac{(1)}{\sigma_B}$	$\frac{(2)}{\sigma_B}$	$\frac{(3)}{\sigma_B}$
M_H	68.4829	37.55	17.55	11.15	0.548	0.256	0.163
$M_H+\Gamma$	13.6962	10.47	13.76	10.44	0.764	1.005	0.761
$M_H-\Gamma$	13.6969	7.49	12.07	9.71	0.547	0.881	0.709

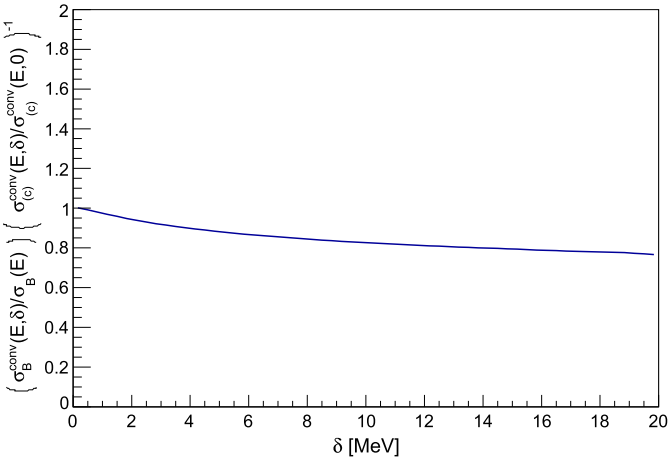

Fig. 7. Numerical cross-check of the validity of the approximation shown in eq. (4.2) for $E = M_H$.

electron collider case with $\delta = 4$ MeV) and for $\delta = 4.2$ MeV it is equal 0.256.[5]

6. Summary

The influence of the QED ISR and the centre-of-mass energy spread on the resonant Higgs boson production cross section, the so-called Higgs line-shape were analyzed numerically in the process $e^+e^- \to H$ and $\mu^+\mu^- \to H$.

It was found that for an electron collider, the QED ISR reduces the peak cross section by factor 0.348. The QED higher order uncertainty of the results was estimated to be below 0.3%. The proper double convolution of the QED radiative spectrum with the centre-of-mass energy spread was performed and doubly cross-checked. For instance, a centre-of-mass energy spread of the same size as the Higgs width ($\delta \simeq 4$ MeV) reduces the Higgs production cross section further down to $0.170\sigma_B$. These results are compatible with (albeit slightly different from) those in the preliminary analysis shown at the recent FCCee workshop, see [4]. They form a solid basis for any analysis of the observability of the Higgs resonant cross section in future e^+e^- colliders.

The same analysis was also repeated for the muon colliders, where the reduction factor due to QED ISR at the peak position was found to be 0.548 and, for instance, gets reduced further down to 0.163 for a centre-of-mass energy spread equal to twice the Higgs width.

Acknowledgements

We would like to thank anonymous Referee for many valuable suggestions that improve the paper and Scott A. Yost for careful proofreading.

Appendix A. Non-uniqueness of the Breit–Wigner formula

In this short Appendix, we want to comment on the issue of the form of the non-uniqueness of the Breit–Wigner formula (2.1) and we shall show that for an extremely narrow Higgs boson resonance this non-uniqueness is numerically completely irrelevant.

The literature on this question is numerous, for instance in the context of the precision measurements of the Z and W boson production and decay, the reader may consult Refs. [22–25]. In particular the use of the complex energy poles of the propagator of virtual particles as a natural solution was advocated, see Ref. [25].

Following Ref. [22] (eqs. (1.6) through (1.9)), the Born term corresponding to (2.1) is

$$\sigma_B(s) \sim \frac{s}{(s-M_H^2)^2+G^2}. \tag{A.1}$$

In case of constant width $G = M_H^2\gamma_H = 525.38$ where $\gamma_H = \frac{\Gamma_H}{M_H} = 3.36\cdot 10^{-5}$, while for the s dependent one we have $G = G(s) = s\gamma_H$. The maximum of the cross section is at

$$\sqrt{s_0} = E_0 = M_H(1+\gamma_H^2)^{1/4} \simeq M_H\left(1+\frac{\gamma_H^2}{4}\right) = 125.090000035\ \text{GeV} \tag{A.2}$$

for the fixed width and

$$E_0 = M_H(1+\gamma_H^2)^{-1/4} \simeq M_H\left(1-\frac{\gamma_H^2}{4}\right) = 125.08999996\ \text{GeV} \tag{A.3}$$

[5] This agrees with the 0.25 result in Ref. [7] for $\delta = 4$ MeV, obtained from an approximate analytical formula.

for the s-dependent width. The difference between E_0 in the above two cases may be regarded as 7×10^{-8} GeV. To our knowledge it is practically impossible to achieve an energy resolution in accelerators of that order of magnitude.

Finally, the formula with the so-called running width (for different variants of Breit–Wigner see, e.g., [26] and references therein) reads

$$\sigma_B(s) \sim \frac{1}{(s-M_H^2)^2+G^2}, \tag{A.4}$$

where $G = s\gamma_H$. The maximum of the cross section is at

$$\sqrt{s_H} = \frac{M_H}{\sqrt{1+\gamma_H^2}} \simeq M_H\Big(1-\frac{\gamma_H^2}{2}\Big), \tag{A.5}$$

which, as above, is beyond measurability in any future accelerator experiment.

Appendix B. Approximate formulas for QED ISR

Starting from eq. (2.2) we are going to provide a very simple approximate formula that allows us to estimate the suppression factor of the peak cross section at $s = M_H^2$ due to QED ISR corrections, thus providing a quick/easy cross-check of more sophisticated numerical calculations.

In the most simplified soft photon approximation, the ISR formula of eq. (2.2) at $E = M_H$ reads

$$\sigma(M_H) \approx \int_0^1 \gamma v^{\gamma-1} \sigma_B(M_H^2(1-v))dv. \tag{B.1}$$

It is a well known fact that the Breit–Wigner profile drops sharply around $|s-M_H^2| = \Gamma_H^2$ and one may therefore approximate it by the following rectangular shape:

$$\sigma_B(s) \simeq \sigma_B(M_H^2)\theta(|s-M_H^2| < \Gamma_H^2),$$

which translates into an integration limit $v \le \Gamma_H/M_H$. As a result, we obtain the following approximate suppression factor for ISR corrections:

$$r_{ISR} = \frac{\sigma_I(M_H^2)}{\sigma_B(M_H^2)} \simeq \frac{1}{\sigma_B(M_H^2)} \int_0^{\frac{\Gamma_H}{M_H}} \gamma v^{\gamma-1} \sigma_B(M_H^2)dv = \left(\frac{\Gamma_H}{M_H}\right)^{\gamma} \tag{B.2}$$

For e^+e^- colliders with $\gamma = 0.1106$, the ISR suppression factor is then estimated to be

$$r_{ISR} = 0.3199. \tag{B.3}$$

This agrees reasonably well with the exact ISR factor of 0.347 seen in Table 1. The relative error of the approximate formula is about 8%.[6] For a $\mu^+\mu^-$ collider with smaller $\gamma = 0.0611$, an approximate ISR suppression factor

$$r_{ISR} = 0.5329, \tag{B.4}$$

is obtained, to be compared with the corresponding value of 0.548 in Table 3. The relative error of the approximate formula is now merely 3%.

References

[1] CMS Collaboration, S. Chatrchyan, et al., Phys. Lett. B 716 (2012) 30.
[2] ATLAS Collaboration, G. Aad, et al., Phys. Lett. B 716 (2012) 1.
[3] CMS Collaboration, S. Chatrchyan, et al., J. High Energy Phys. 1306 (2013) 081, arXiv:1303.4571.
[4] D. d'Enterria, G. Wojcik, R. Aleksan, Presentation at 8 FCC-ee Physics Workshop, 2014.
[5] S. Jadach, B.F.L. Ward, Z. Was, Phys. Rev. D 63 (2001) 113009, arXiv:hep-ph/0006359.
[6] S. Dittmaier, A. Kaiser, Phys. Rev. D 65 (2002) 113003, arXiv:hep-ph/0203120.
[7] M. Greco, arXiv:1503.05046, 2015.
[8] Michael E. Peskin, Dan V. Schroeder, An Introduction to Quantum Field Theory, Westview Press, 1995.
[9] G. Aad, et al., ATLAS Collaboration, CMS Collaboration, Phys. Rev. Lett. 114 (2015) 191803, arXiv:1503.07589 [hep-ex].
[10] J. Beringer, et al., Status of Higgs Boson Physics, 2012, and 2013 update for the 2014 edition.
[11] K.A. Olive, et al., Status of Higgs Boson Physics, 2014.
[12] S. Jadach, B.F.L. Ward, Comput. Phys. Commun. 56 (1990) 351.
[13] S. Jadach, M. Skrzypek, M. Martinez, Phys. Lett. B 280 (1992) 129.
[14] S. Jadach, B. Pietrzyk, M. Skrzypek, Phys. Lett. B 456 (1999) 77.
[15] S. Jadach, M. Skrzypek, B. Ward, Phys. Lett. B 257 (1991) 173.
[16] M. Skrzypek, S. Jadach, M. Martinez, W. Płaczek, Z. Was, Phys. Lett. B 372 (1996) 289.
[17] I. Antcheva, et al., in: 40 YEARS OF CPC: a celebratory issue focused on quality software for high performance, grid and novel computing architectures, Comput. Phys. Commun. 180 (2009) 2499.
[18] S. Jadach, Comput. Phys. Commun. 130 (2000) 244, arXiv:physics/9910004.
[19] S. Jadach, Comput. Phys. Commun. 152 (2003) 55, arXiv:physics/0203033.
[20] M. Slawinska, S. Jadach, Comput. Phys. Commun. 182 (2011) 748, arXiv:1006.5633.
[21] MAP Collaboration, MICE Collaboration, D.M. Kaplan, EPJ Web Conf. 95 (2015) 03019, arXiv:1412.3487.
[22] D.Y. Bardin, A. Leike, T. Riemann, M. Sachwitz, Phys. Lett. B 206 (1988) 539.
[23] R.G. Stuart, Phys. Lett. B 262 (1991) 113.
[24] R.G. Stuart, Phys. Lett. B 272 (1991) 353.
[25] S. Dittmaier, et al., arXiv:1201.3084, 2012.
[26] C. Anastasiou, S. Buehler, F. Herzog, A. Lazopoulos, J. High Energy Phys. 1204 (2012) 004, arXiv:1202.3638.

[6] Sometimes one expands further $r_{ISR} \simeq 1 - \gamma \ln(\Gamma_H/M_H)$ but this makes sense only for $r_{ISR} > 0.5$, which is not our case.